Current-driven domain wall motion along high perpendicular anisotropy multilayers: The role of the Rashba field, the spin Hall effect, and the Dzyaloshinskii-Moriya interaction

Eduardo Martinez, Satoru Emori, and Geoffrey S. D. Beach

Citation: Appl. Phys. Lett. **103**, 072406 (2013); doi: 10.1063/1.4818723
View online: http://dx.doi.org/10.1063/1.4818723
View Table of Contents: http://apl.aip.org/resource/1/APPLAB/v103/i7
Published by the AIP Publishing LLC.

Current-driven domain wall motion along high perpendicular anisotropy multilayers: The role of the Rashba field, the spin Hall effect, and the Dzyaloshinskii-Moriya interaction

Eduardo Martinez,[1,a)] Satoru Emori,[2] and Geoffrey S. D. Beach[2]
[1]*Dpto. Fisica Aplicada, Universidad de Salamanca, Plaza de los Caidos s/n, E-38008, Salamanca, Spain*
[2]*Department of Materials Science and Engineering, Massachusetts Institute of Technology, Cambridge, Massachusetts 02139, USA*

(Received 30 May 2013; accepted 29 July 2013; published online 15 August 2013)

The current-induced domain wall motion along a thin cobalt ferromagnetic strip sandwiched in a multilayer (Pt/Co/AlO) is theoretically studied with emphasis on the roles of the Rashba field, the spin Hall effect, and the Dzyaloshinskii-Moriya interaction. The results point out that these ingredients, originated from the spin-orbit coupling, are consistent with recent experimental observations in three different scenarios. With the aim of clarifying which is the most plausible the influence of in-plane longitudinal and transversal fields is evaluated. © *2013 AIP Publishing LLC*. [http://dx.doi.org/10.1063/1.4818723]

The current-induced domain wall motion (CIDWM) along thin ferromagnetic layers with high perpendicular magnetoscrystalline anisotropy sandwiched between a heavy metal and an oxide has been demonstrated to be very efficient,[1–4] and it promises unprecedented opportunities for developing spintronic devices.[5] Apart from its technological interest, the CIDWM along these asymmetric stacks is also of fundamental relevance because it is related to interesting physics phenomena. The CIDWM is often explained in terms of the standard adiabatic and non-adiabatic spin-transfer torques (STTs).[6,7] However, the domain wall (DW) moves along the current (against the electron flow) in Pt/Co/AlO (Ref. 1) and in Pt/CoFe/MgO (Ref. 3) stacks, an observation which is contrary to the standard STT unless the polarization factor P or the non-adiabatic parameter ξ are negative. Moreover, the addressed high velocity in these asymmetric stacks is not consistent with the STT, and recent experimental observations[1,8] pointed out that in the presence of structural inversion asymmetry and/or heavy metals like Pt,[1,2,9] strong spin-orbit coupling (SOC) can lead to additional spin-orbit torques (SOTs) qualitatively different from the STTs. These SOTs could, at least, be originated by two phenomena: the Rashba effect due to the large SOC and structure inversion asymmetry at the two different heavy-metal/ferromagnet and ferromagnet/oxide interfaces[10–14] and/or the spin Hall current generated from the heavy metal layer and injected in the thin ferromagnet.[15–21] On the other hand, a thin ferromagnetic layer in contact with a heavy-metal with strong SOC is expected to experience an interfacial anisotropic exchange due to the Dzyaloshinskii-Moriya interaction (DMI).[22–29] The DMI is a chiral spin-orbit interaction originating from relativistic effects that occur due to the lack of inversion symmetry of the atomic structure, and it can result in topologically rich magnetization patterns such as spiral, skyrmions[25,27,28] or chiral domain walls.[29] In particular, it has been recently pointed out that in a thin ferromagnetic layer sandwiched between a heavy-metal and an oxide, the DMI stabilizes chiral DWs of Neel type which are efficiently driven by the spin Hall effect (SHE).[3,30] Given the broad interest on the CIDWM in these heavy-metal/ferromagnet/oxide heterostructures, it is crucial to reveal the underlaying physics of all these SOC effects.

In this paper, the experimental data by Miron *et al.*[1] for the CIDWM in a Pt/Co/AlO stack are taken as reference to provide different explanations which could be theoretically consistent with. Based on the experimental available works and by using the one-dimensional model, we find and describe three possible scenarios consistent with this highly efficient CIDWM along the current by considering different combinations of STTs, Rashba and spin Hall SOTs, and DMI.

In order to mimic the experimental results by Miron and co-workers[1] for a Co strip with a cross section of $L_y \times L_z = 500\,\text{nm} \times 0.6\,\text{nm}$ sandwiched between Pt and AlO layers, the following parameters were adopted:[1] saturation magnetization $M_s = 1.09 \times 10^6\,\text{A/m}$, exchange constant $A = 10^{-11}\,\text{J/m}$, uniaxial anisotropy constant $K_u = 1.19 \times 10^6\,\text{J/m}^3$, and damping $\alpha = 0.2$.[33] Under instantaneous injection of a spatially uniform current density along the x-axis $\vec{j}_a = j_a \vec{u}_x$, the magnetization dynamics is governed by the augmented Landau-Lifshitz Gilbert equation

$$\frac{d\vec{m}}{dt} = -\gamma_0 \vec{m} \times \vec{H}_{eff} + \alpha\left(\vec{m} \times \frac{d\vec{m}}{dt}\right) + \vec{\tau}_{ST} + \vec{\tau}_{SO}, \quad (1)$$

where $\vec{m}(\vec{r}, t) = \vec{M}(\vec{r}, t)/M_s$ is the normalized local magnetization, γ_0 is the gyromagnetic ratio, and α the Gilbert damping parameter. $\vec{H}_{eff}$ is effective field, which apart from the standard exchange, magnetostatic, uniaxial anisotropy and Zeeman contributions also includes the DMI[22–24]

$$\vec{H}_{DMI} = -\frac{1}{\mu_0 M_s}\frac{\delta \epsilon_{DMI}}{\delta \vec{m}}, \quad (2)$$

where ϵ_{DMI} is the DMI energy density[24] given by[30]

$$\epsilon_{DMI} = D[m_z \nabla \cdot \vec{m} - (\vec{m} \cdot \nabla) m_z] \quad (3)$$

a)Author to whom correspondence should be addressed. Electronic mail: edumartinez@usal.es

and D is the DMI parameter describing its intensity. The STT $\vec{\tau}_{ST}$ is given by[6,7]

$$\vec{\tau}_{ST} = b_J(\vec{u}_x \cdot \nabla)\vec{m} - \xi b_J \vec{m} \times (\vec{u}_x \cdot \nabla)\vec{m}, \tag{4}$$

where $b_J = j_a \frac{\mu_B P}{eM_s}$ with μ_B the Bohr magneton and $e < 0$ the electron's charge. Finally, $\vec{\tau}_{SO}$ describes the SOTs, which includes Rashba and spin Hall contributions

$$\vec{\tau}_{SO} = -\gamma_0 \vec{m} \times \vec{H}_R + \eta\gamma_0 \xi \vec{m} \times (\vec{m} \times \vec{H}_R) + \gamma_0 \vec{m} \times (\vec{m} \times H_{SH}\vec{u}_y), \tag{5}$$

where two contributions from the Rashba effect (1st and 2nd terms in Eq. (5)) and one from the spin Hall effect (3rd term in Eq. (5)) can be identified. In the presence of the Rashba interaction, the charge current flowing in the thin ferromagnetic layer in a direction parallel to the interfaces generates a spin accumulation that can interact with the local magnetization via an exchange coupling mediated by a Rashba effective field $\vec{H}_R = H_R\vec{u}_y$ given by[1,11,12]

$$\vec{H}_R = \frac{\alpha_R P}{\mu_0 \mu_B M_s}(\vec{u}_z \times \vec{j}_a) = \frac{\alpha_R P j_a}{\mu_0 \mu_B M_s}\vec{u}_y, \tag{6}$$

with α_R being the Rashba parameter. Other Rashba SOT could also arise either from the spin diffusion inside the magnetic layer or from a spin current associated to Rashba interaction at the interfaces with the spin-orbit metal.[14] These phenomena have been predicted to contribute to the SOT by means of an additional non-adiabatic contribution to the Rashba SOT,[13,14] which is proportional to the non-adiabatic parameter ξ (2nd terms in Eq. (5)). Another possible source of SOT originates from the SHE.[15,16] In a typical multilayer stack, a spin current can be generated by the SHE in the heavy non-magnetic metal layers such as Pt. This spin current can be injected into the ferromagnetic layer, resulting in an additional SOT (3rd term in Eq. (5)), with amplitude H_{SH} given by[18–21]

$$H_{SH} = \frac{\hbar\theta_{SH} j_a}{\mu_0 2eM_s L_z} = \frac{\mu_B \theta_{SH} j_a}{\gamma_0 eM_s L_z}, \tag{7}$$

where L_z is the thickness of the ferromagnetic layer, θ_{SH} is the Spin Hall angle, which is defined as the ratio between the spin current and the charge current densities. Here, the factor η was considered to account ($\eta = 1$) or not ($\eta = 0$) the Slonczewski-like torque due to the Rashba effect. On the other hand, the SHE results in a Slonczewski-like torque (3rd term at the rhs in Eq. (5)).

The one-dimensional model (1DM), assumes that (i) the magnetization varies only in the direction of the strip (here x-axis, $\vec{m}(x,t)$) and that (ii) the static DW profile is essentially preserved during its motion. In this 1DM, the extended LLG Eq. (1) can be integrated over the static DW profile,[3,6,7,30] and therefore, the CIDWM, including STTs, SOTs, and DMI, is described by two coupled equations

$$\frac{\dot{X}}{\Delta} = \alpha\gamma_0' H - \frac{\gamma_0' H_K}{2}\sin(2\Phi) + \frac{(1+\alpha\xi)}{1+\alpha^2}\frac{b_J}{\Delta} + \frac{\pi}{2}\gamma_0'[-(1+\alpha\xi\eta)H_R + \alpha H_{SH} - H_y]\cos(\Phi) + \frac{\pi}{2}\gamma_0'[H_D + H_x]\sin(\Phi), \tag{8}$$

$$\dot{\Phi} = \gamma_0' H + \alpha\frac{\gamma_0' H_K}{2}\sin(2\Phi) + \frac{(\xi-\alpha)}{1+\alpha^2}\frac{b_J}{\Delta} + \frac{\pi}{2}\gamma_0'[-(\eta\xi-\alpha)H_R + H_{SH} + \alpha H_y]\cos(\Phi) - \alpha\frac{\pi}{2}\gamma_0'[H_D + H_x]\sin(\Phi), \tag{9}$$

where $\gamma_0' = \gamma_0/(1+\alpha^2)$, $X = X(t)$ is the DW position, and $\Phi = \Phi(t)$ is the DW angle, which is defined as the in-plane (x-y) angle with respect to the positive x-axis: $\Phi(0) = 0, \pi$ for Neel DW, and $\Phi(0) = \pi/2, 3\pi/2$ for Bloch DW configurations. Positive current ($j_a > 0$) is along the positive x-axis, Δ is the DW width, and H_K is the hard-axis anisotropy field of magnetostatic origin. The DW width is estimated to be $\Delta = \sqrt{A/K_u} \approx 3\,\text{nm}$, and the shape anisotropy field is given $H_K = N_x M_s$, where N_x is the magnetostatic factor given by[34] $N_x = L_z Log(2)/(\pi\Delta) = 0.044$. $H_D = D/(\mu_0 M_s \Delta)$ is the DMI effective field pointing along the x-axis inside the DW.[30] The applied field has Cartesian components (H_x, H_y, H_z). The total field $H = H_z + H_p(X) + H_{th}(t)$ includes (i) the applied magnetic field along the easy z-axis (H_z), (ii) the spatial dependent pinning field ($H_p(X)$), which accounts for local imperfections and can be derived from an effective spatial-dependent pinning potential $V_{pin}(X)$ as $H_p(X) = -\frac{1}{2\mu_0 M_s L_y L_z}\frac{\partial V_{pin}(X)}{\partial X}$, and (iii) the thermal field ($H_{th}(t)$), which describes the effect of thermal fluctuations.[31,32]

In order to explain the experimental results by Miron and co-workers,[1] several combinations of STTs, SOTs, and DMI have been evaluated. In the following discussion, the possible ones consistent with the highly efficient CIDWM along the current are described.

Scenario 1. The experimental observations by Miron and co-workers[1] indicates a DW motion (CIDWM) along the current, reaching velocities around 400 m/s for $j_a \approx 3 \times 10^{12}\text{A/m}^2$. This high efficiency was interpreted by the authors by suggesting that a strong Rashba field stabilizes the Bloch DW configuration and supports the standard STT with both a high polarization factor ($P \sim 1$) and non-adiabaticity ($\xi \sim 1$). However, the standard STT considers that both $P > 0$ and $\xi > 0$ are positive quantities predicting a DWM against the current (along the electron flow). The experimental observations could be in principle consistent with this scenario (strong Rashba field supporting the STT) if one of them (P or ξ) is a negative value. For example, it has theoretically suggested that in very narrow walls, the non-adiabaticity could change its sign.[35,36] Therefore, here we have explored this scenario by considering a similar value of the Rashba parameter as suggested in Ref. 38 ($\alpha_R = 10^{-10}\,\text{eVm}$ with $\eta = 0$) along with the standard STTs with $P = 0.5$ and $\xi = -1$. The 1DM predictions for the DW velocity and the terminal DW angle are shown in Figs. 1(a) and 1(b) and compared to the experimental data by Miron and co-workers[1] (blue squares). The experimental results for the DW velocity depict a low-current creep regime and a

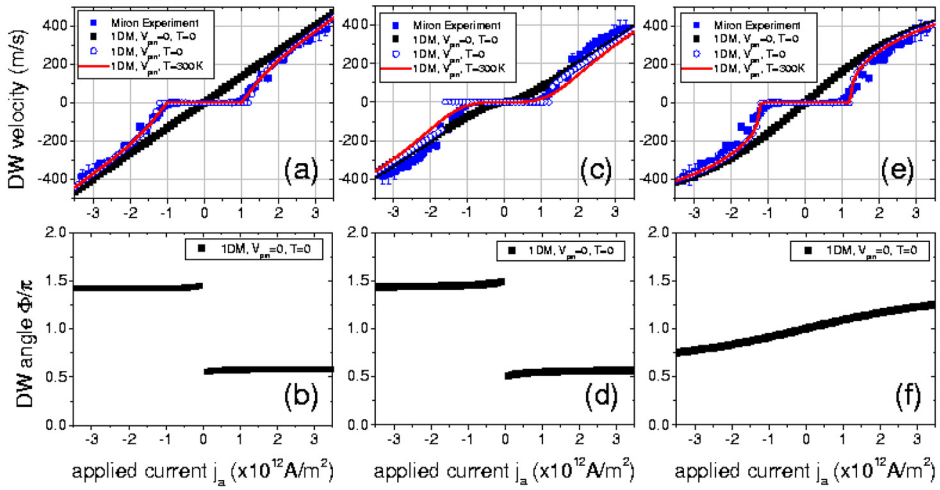

FIG. 1. DW velocity and DW angle as a function of the applied density current in three different scenarios: (a), (b) STT with $P = 0.5$ and $\xi = -1$ and Rashba field with $\alpha_R = 10^{-10}$ eVm and $\eta = 0$; (c), (d) STT with $P = 0.5$ and $\xi = +0.1$, Rashba field with $\alpha_R = 10^{-10}$ eVm and $\eta = 1$, and SHE with $\theta_{SH} = 0.13$; (e), (f) DMI with $D = -2.4\,\mathrm{mJ/m^2}$ and SHE with $\theta_{SH} = 0.08$. Blue squares correspond to the experimental data by Miron.[1] Black squares are the 1DM predictions for a perfect strip at zero temperature. Open circles are the 1DM results considering a rough sample ($V_{pin} \neq 0$) at zero temperature, and red lines are the 1DM results considering a rough sample ($V_{pin} \neq 0$) at room temperature ($T = 300\,\mathrm{K}$). The simulated pinning potential is given by $V_{pin}(X) = V_0 \sin^2(\pi X/p)$. The periodicity of the pinning landscape is $p = 30\,\mathrm{nm}$, and the amplitude is $V_0 = 1.8 \times 10^{-20}$ J, $V_0 = 6 \times 10^{-20}$ J, and $V_0 = 50 \times 10^{-20}$ J for the cases (a), (b), and (c), respectively. A positive velocity indicates a DW motion along the $x > 0$ axis that is along the direction of the positive current.

high-current flow regime. The first one is dominated by the balance between the driving force (STT) and the local pinning potential due to the imperfections which oppose to the free DW motion. For very low currents, the DW does not move because the driving current is still very small to overcome the local energy barrier induced by local pinning. As the current increases, the DW motion is thermally activated, and the DW velocity increases exponentially, a typical behavior of the thermally activated DW motion in the creep regime.[37] For very high current, the DW reaches the flow regime where pinning, and thermal effects play a negligible role.[37] Therefore, the DW velocity in this high-current flow regime can be fitted by the 1DM in the absence of pinning and thermal effects if the key parameters (P, ξ, and α_R) are properly chosen, as it is the case of the black squares in Fig. 1(a), where $V_{pin} = 0$ and $T = 0$. As it is shown in Fig. 1(b), the DW configuration is of Bloch type: the internal DW magnetization points along the positive transversal y-axis for positive currents ($\Phi \approx +\pi/2$) or along the negative transversal y-axis for negative currents ($\Phi \approx 3\pi/2$) as it is expected from Eq. (6). The inclusion of pinning ($V_{pin} \neq 0$) in the 1DM (with $V_0 = 1.8 \times 10^{-20}$ J and $p = 30\,\mathrm{nm}$), both at zero temperature ($T = 0$, open circles in Fig. 1(a)) and at room temperature ($T = 300\,\mathrm{K}$, solid red line in Fig. 1(a)), provides a more realistic description of the full experimental results. Note that the flow regime, which is the relevant one to extract the key parameters, does not change substantially with respect to the perfect case.

Scenario 2. Although it has been theoretically predicted that the non-adiabatic parameter could be negative in narrow walls,[35,36] the experimental verification has not been established. Moreover, it has been experimentally demonstrated that the SHE-driven spin accumulation at the heavy-metal/ferromagnet interface generates a Slonczewski-like torque strong enough to switch uniformly magnetized films.[18,19] Apart from the Slonczewski-like torque due to the SHE, the theoretical work by Wang and Manchon[14] indicates that also the Rashba field could contribute to the Slonczewski-like torque, which enters as a correction proportional to the non-adiabaticity.[13] Here, it has been verified that considering both the field-like and Slonczewski-like torques due to the Rashba ($\eta = 1$) along with the Slonczewski-like torque due to the SHE ($\theta_{SH} = 0.13$), the experimental results[1] can be also reproduced if a small and positive non-adiabatic parameter ($\xi = +0.1$) is taken into account (Fig. 1(c)). Note that the deduced value for the spin Hall angle ($\theta_{SH} = 0.13$) is in good agreement with experimental measurements.[17–19] Also in this scenario, the internal DW adopts an internal magnetization close to the Bloch type which again is mainly related to the strong Rashba field-like torque (Fig. 1(d)). Although now the non-adiabaticity is positive and considerably small than in the former scenario, a high value of the Rashba parameter ($\alpha_R = 10^{-10}$ eVm) is still required to achieve the fit. However, several experimental works[3,19] have pointed out that the Rashba field is indeed around two orders of magnitude smaller than the used here ($\alpha_R = 10^{-10}$ eVm (Ref. 38)). Note also that although it is not depicted here, it was verified that by reducing the Rashba parameter by one order of magnitude ($\alpha_R = 10^{-11}$ eVm), the direction of DW motion reverses being along the electron flow, in contradiction to the experiments (for such a low Rashba field, the STT dominates for all tested values of $0 < \xi < 20\alpha$ and $0 < \theta_{SH} < 0.2$).

Scenario 3. Apart from the high Rashba parameter required by previous scenarios, they are only in agreement with the experimental observations in the presence of the standard STT. However, current-induced DW motion is absent in symmetric Pt/Co/Pt stacks,[2,39–41] and semi-classical transport calculations[41] suggest that spin-polarized current in the ultrathin (<1 nm) Co layer is vanishingly small. A recent work by Tanigawa *et al.*[42] has also shown the vanishing polarization for thinner Co layer in a Co/Ni system. Therefore, in the absence of STT, the Rashba field-like torque (1st term in Eq. (5)) only stabilizes the Bloch DW configuration, but it lacks the correct symmetry to drive

DWs directly. Note also that if the polarization factor is indeed close to zero ($P \approx 0$) for thin Co layers, both field-like and Slonczewski-like torque contributions due to the Rashba field will be also vanishingly small or null. On the contrary, the SHE is not proportional to P, but its Slonczewski-like torque (3rd term in Eq. (5)) would result to be zero for a perfect Bloch DW configuration.[43] Due to magnetostatics considerations,[44] the Bloch configuration is expected to be the energetically favored state in most of the experimental studies. Although deviations from the pure Bloch state could be induced by field misalignments, small contributions from the STT or from shape anisotropy in narrow wires,[8] up-down and down-up DWs would be driven in opposite directions. Therefore, SHE alone cannot drive trains of DWs in the same direction,[8] and it alone is not capable to explain the current-driven DW motion in Pt/Co/AlO and similar stacks. As recently pointed out by Emori *et al.*,[3] the additional ingredient is the DMI, which has been theoretical shown to promote chiral Neel DWs as a consequence of the anisotropy exchange between the magnetic moments and the interfacial atoms with high SOC.[22–27,29] Indeed, the current-driven DW motion in heavy-metal/ferromagnet/oxide structures is naturally explained by the combination of the SHE, which produces the main current-induced torque, and the DMI, which stabilizes chiral Neel DWs whose symmetry permits uniform motion with very high efficiency.[3] Here we show that this scenario (SHE along with DMI) is indeed quantitatively consistent with the experimental results by Miron.[1] The 1DM results for $\theta_{SH} = 0.08$ and $D = -2.4\,\mathrm{mJ/m^2}$ are compared to the experimental values in Fig. 1(e). Contrary to former scenarios, now the Rashba and the STT are zero. The up-down DW configuration under zero current is of Neel type ($\Phi = \pi$) with its internal magnetization pointing mainly along the negative x-axis due to the negative value of the DMI (Fig. 1(f)). For finite currents, the DW deviates from the perfect Neel state, and it tends to reach an intermediate state between Bloch and Neel states for very high currents: $\Phi \to \pi/4$ for very high positive currents and $\Phi \to 5\pi/4$ for negative currents.

The results of Fig. 1 indicate that in principle the three scenarios could be consistent with the experimental results. In order to elucidate if one of them is indeed describing the physics governing the current-driven DW motion in these asymmetric stacks, the influence of in-plane fields, along the longitudinal x-axis or along the transversal y-axis, have been studied by the 1DM considering a perfect sample at zero temperature. The transversal field ($\vec{B}_y = \mu_0 H_y \vec{u}_y$) points in the same direction than the Rashba field ($\vec{B}_R = \mu_0 H_R \vec{u}_y$), supporting or opposing to it depending on its sign. The longitudinal field ($\vec{B}_x = \mu_0 H_x \vec{u}_x$) points in the same direction than DMI ($\vec{B}_D = \mu_0 H_D \vec{u}_x$). The results for the three scenarios are depicted in Fig. 2 under a fixed current of $j_a = 10^{12}\,\mathrm{A/m^2}$. Due to the strong Rashba field considered in the scenario 1 ($B_R \approx 791\,\mathrm{mT}$), the current-driven DW velocity is not modified by the in-plane fields (Fig. 2(a)). When the SHE is taken into account along with the STT and the Rashba field (scenario 2, the DW reaches a saturation velocity with different signs under strong longitudinal fields with opposite polarities (see Fig. 2(b)). These strong longitudinal field promote the Neel DW configuration which is mainly driven by the SHE. Under transversal fields, the DW velocity also experiences a change of sign around $B_y \approx 60\,\mathrm{mT}$ which is approximately the value of the SHE effective field H_{SH} given by Eq. (7). For strong transversal fields the DW adopts a Bloch state and the velocity tends to vanish because of the low non-adiabaticity. Finally, under the only action of SHE and DMI (scenario 3), the negative (positive) longitudinal field supports (opposes) the DMI field (see Fig. 2(c)). In the absence of in-plane field ($B_x = B_y = 0$), the DW state is of Neel type with internal magnetization pointing to the left ($\Phi \approx \pi$) due to the negative value of the DMI. The DW velocity saturates under strong negative longitudinal fields, but it decreases under positive longitudinal fields which oppose to the DMI. Under very strong B_x (not shown), the internal DW magnetization reverses pointing to the right ($\Phi \approx 0$), and this change in the DW chirality produces also a reversal on the DW motion (see supplementary material in Ref. 3). Transversal fields also modify the DW velocity in this scenario. For transversal fields with $|B_y| > 200\,\mathrm{mT}$, the DW velocity decreases monotonously because the internal DW magnetization starts to deviate from the pure Neel state. Under very strong transversal fields (not shown) the DW velocity tends to zero because the DW configuration adopts a Bloch state which cannot be driven by the SHE. It is worthy to note that although our former experimental study was conducted in the thermally activated regime in a slightly different material system,[3] it qualitatively shows the same behavior than the predicted results of the scenario 3 (Fig. 2(c)), and it is definitely not consistent with Fig. 2(a) (scenario 1) or Fig. 2(b) (scenario 2) studied here.

Some preliminary micromagnetic simulations have been also carried out for the same experimental cross section (with $L_y = 500\,\mathrm{nm}$ and $L_z = 0.6\,\mathrm{nm}$), indicating that under strong in-plane fields not only the internal DW moment is

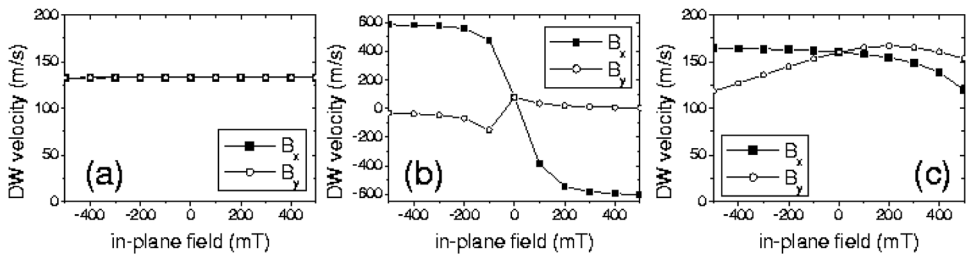

FIG. 2. Current-driven DW velocity as a function of the in-plane fields (black squares B_x, open circles B_y) predicted by the 1DM for a perfect sample at zero temperature. Three different scenarios are studied: (a) scenario 1: STT with $P = 0.5$ and $\xi = -1$, and Rashba field with $\alpha_R = 10^{-10}$ eVm and $\eta = 0$; (b) scenario 2: STT with $P = 0.5$ and $\xi = +0.1$, Rashba field with $\alpha_R = 10^{-10}$ eVm and $\eta = 1$, and SHE with $\theta_{SH} = 0.13$; (c) scenario 3: DMI with $D = -2.4\,\mathrm{mJ/m^2}$ and SHE with $\theta_{SH} = 0.08$. The applied current is $j_a = 10^{12}\,\mathrm{A/m^2}$ in all cases.

rotated toward to the field but also the DW plane is eventually tilted and the magnetization in the domains slightly deviates from the z-axis (not shown here). These two last issues cannot be accounted by the simple 1DM used here, and therefore full micromagnetic simulations are need to completely describe the influence of in-plane fields on the current-induced DW motion by the SHE in the presence of DMI (scenario 3). However, such a full micromagnetic analysis of these issues will require a substantial computational effort and is beyond the scope of the present work. This study is currently being performed, and the results will be addressed elsewhere.[45] In the meanwhile, the 1DM results of Fig. 2 have to be considered as a first approach valid for the low-field range. Indeed, the 1DM results reproduce quite accurately the full micromagnetic simulations in strips with reduced width (see supplementary material for a compared micromagnetic and 1DM analysis).[46]

In summary, three different scenarios seem to be consistent with recent experimental observations in the high-current flow regime, where the DW propagates along the current with high efficiency. In the first case, a strong Rashba field stabilizes the Bloch configuration which is propagated by the spin transfer torque if a negative non-adiabaticity is considered. Similar results are also obtained for positive non-adiabaticity if both Rashba and spin Hall contributions to the Slonczewski-like torque are included along with the Rashba field-like torque. The third possibility indicates that, even in the absence of both Rashba and spin-transfer torques, the DW can be driven along the current by the Slonczewski-like spin Hall torque if the Neel DW configuration with a given chirality is adopted as due to the Dzyaloshinskii-Moriya interaction. From our fitting, a strong Dzyaloshinskii-Moriya interaction was inferred ($D = -2.4\,\mathrm{mJ/m^2}$) considering similar spin Hall angle as the one directly measured in switching experiments.[3] With the aim of providing other test for the experiments, the influence of in-plane field on the current-driven DW velocity has been also analyzed. This study could be useful to elucidate which are the real and dominant mechanisms governing the underlying physics behind the current-driven DW motion along asymmetric stacks.

The authors would like to thank M. Miron and G. Gaudin for providing their experimental data. This work was supported by project MAT2011-28532-C03-01 from Spanish Government and project SA163A12 from JCyL.

[1]I. M. Miron, T. Moore, H. Szambolics, L. D. Buda-Prejbeanu, S. Auffret, B. Rodmacq, S. Pizzini, J. Vogel, M. Bonfim, A. Schuhl, and G. Gaudin, Nature Mater. **10**, 419 (2011).
[2]S. Emori, D. C. Bono, and G. S. D. Beach, Appl. Phys. Lett. **101**, 042405 (2012).
[3]S. Emori, U. Bauer, S.-M. Ahn, E. Martinez, and G. S. D. Beach, Nature Mater. **12**, 611 (2013).
[4]K.-S. Ryu, L. Thomas, S.-H. Yang, and S. S. P. Parkin, Appl. Phys. Express **5**, 093006 (2012).
[5]S. S. P. Parkin, M. Hayashi, and L. Thomas, Science **320**, 190 (2008).
[6]S. Zhang and Z. Li, Phys. Rev. Lett. **93**, 127204 (2004).
[7]A. Thiaville, Y. Nakatani, J. Miltat, and Y. Suzuki, Europhys. Lett. **69**, 990 (2005).
[8]P. P. J. Haazen, E. Mure, J. H. Franken, R. Lavrijsen, H. J. M. Swagten, and B. Koopmans, Nature Mater. **12**, 299 (2013).
[9]R. Lavrijsen, P. P. Haazen, E. Mure, J. H. Franken, J. T. Kohlhepp, H. J. M. Swagten, and B. Koopmans, Appl. Phys. Lett. **100**, 262408 (2012).
[10]Yu. A. Bychkov and E. I. Rashba, JETP Lett. **39**, 78 (1984).
[11]A. Manchon and S. Zhang, Phys. Rev. B **78**, 212405 (2008); **79**, 094422 (2009).
[12]P. Gambardella and I. M. Miron, Philos. Trans. R. Soc. London, Ser. A **369**, 3175 (2011).
[13]K.-W. Kim, S.-M. Seo, J. Ryu, K.-J. Lee, and H.-W. Lee, Phys. Rev. B **85**, 180404(R) (2012).
[14]X. Wang and A. Manchon, Phys. Rev. Lett. **108**, 117201 (2012).
[15]M. Dyakonov and V. Perel, JETP Lett. **13**, 467 (1971).
[16]J. E. Hirsch, Phys. Rev. Lett. **83**, 1834 (1999).
[17]B. Gu, I. Sugai, T. Ziman, G. Y. Guo, N. Nagaosa, T. Seki, K. Takanashi, and S. Maekawa, Phys. Rev. Lett. **105**, 216401 (2010).
[18]L. Liu, T. Moriyama, D. C. Ralph, and R. A. Buhrman, Phys. Rev. Lett. **106**, 036601 (2011).
[19]L. Liu, C.-F. Pai, Y. Li, H. W. Tseng, D. C. Ralph, and R. A. Buhrman, Science **336**, 555 (2012).
[20]K. Kondou, H. Sukegawa, S. Mitani, K. Tsukagoshi, and S. Kasai, Appl. Phys. Express **5**, 073002 (2012).
[21]S.-M. Seo, K.-W. Kim, J. Ryu, H.-W. Lee, and K.-J. Lee, Appl. Phys. Lett. **101**, 022405 (2012).
[22]T. Moriya, Phys. Rev. Lett. **4**, 228 (1960).
[23]M. Bode, M. Heide, K. von Bergmann, P. Ferriani, S. Heinze, G. Bihlmayer, A. Kubetzka, O. Pietzsch, S. Blugel, and R. Wiesendanger, Nature (London) **447**, 190 (2007).
[24]M. Heide, G. Bihlmayer, and S. Blugel, Phys. Rev. B **78**, 140403 (2008).
[25]X. Z. Yu, Y. Onose, N. Kanazawa, J. H. Park, J. H. Han, Y. Matsui, N. Nagaosa, and Y. Tokura, Nature (London) **465**, 901 (2010).
[26]S. Heinze, K. von Bergmann, M. Menzel, J. Brede, A. Kubetzka, R. Wiesendanger, G. Bihlmayer, and S. Blügel, Nature Phys. **7**, 713 (2011).
[27]S. X. Huang and C. L. Chien, Phys. Rev. Lett. **108**, 267201 (2012).
[28]A. Fert, V. Cros, and J. Sampaio, Nat. Nanotechnol. **8**, 152–156 (2013).
[29]G. Chen, J. Zhu, A. Quesada, J. Li, A. T. N'Diaye, Y. Huo, T. P. Ma, Y. Chen, H. Y. Kwon, C. Won, Z. Q. Qiu, A. K. Schmid, and Y. Z. Wu, Phys. Rev. Lett. **110**, 177204 (2013).
[30]A. Thiaville, S. Rohart, E. Jue, V. Cros, and A. Fert, Europhys. Lett. **100**, 57002 (2012).
[31]E. Martinez, Adv. Condens. Matter Phys. **2012**, 954196 (2012).
[32]E. Martinez and G. Finocchio, IEEE Trans. Magn. **49**(7), 3105 (2013); E. Martinez, G. Finocchio, L. Torres, and L. Lopez-Diaz, AIP Adv. **3**, 072109 (2013).
[33]A. J. Schellekens, L. Deen, D. Wang, J. T. Kohlhepp, H. J. M. Swagten, and B. Koopmans, App. Phys. Lett. **102**, 082405 (2013).
[34]S. V. Tarasenko, A. Stankiewicz, V. V. Tarasenko, and J. Ferre, J. Magn. Magn. Mater. **189**, 19 (1998).
[35]I. Garate, K. Gilmore, M. D. Stiles, and A. H. MacDonald, Phys. Rev. B **79**, 104416 (2009).
[36]S. Bohlens and D. Pfannkuche, Phys. Rev. Lett. **105**, 177201 (2010).
[37]E. Martinez, J. Phys.: Condens. Matter **24**, 024206 (2012).
[38]I. M. Miron, G. Gaudin, S. Auffret, B. Rodmacq, A. Schuhl, S. Pizzini, J. Vogel, and P. Gambardella, Nature Mater. **9**, 230 (2010).
[39]T. A. Moore, I. M. Miron, G. Gaudin, G. Serret, S. Auffret, B. Rodmacq, A. Schuhl, S. Pizzini, J. Vogel, and M. Bonfim, Appl. Phys. Lett. **93**, 262504 (2008).
[40]I. M. Miron, P.-J. Zermatten, G. Gaudin, S. Auffret, B. Rodmacq, and A. Schuhl, Phys. Rev. Lett. **102**, 137202 (2009).
[41]M. Cormier, A. Mougin, J. Ferre, A. Thiaville, N. Charpentier, F. Piechon, R. Weil, V. Baltz, and B. Rodmacq, Phys. Rev. B **81**, 024407 (2010).
[42]H. Tanigawa, T. Suzuki, S. Fukami, K. Suemitsu, N. Ohshima, and E. Kariyada, Appl. Phys. Lett. **102**, 152410 (2013).
[43]A. V. Khvalkovskiy, V. Cros, D. Apalkov, V. Nikitin, M. Krounbi, K. A. Zvezdin, A. Anane, J. Grollier, and A. Fert, Phys. Rev. B **87**, 020402(R) (2013).
[44]E. Martinez, L. Torres, and L. Lopez-Diaz, Phys. Rev. B **83**, 174444 (2011).
[45]S. Emori, E. Martinez, U. Bauer, S.-M. Ahn, P. Agrawal, D. C. Bono, and G. S. D. Beach, "Spin Hall torque magnetometry of Dzyaloshinskii domain walls," arXiv:1308.1432.
[46]See supplementary material at http://dx.doi.org/10.1063/1.4818723 for the comparison of one-dimensional model results (1DM) to full micromagnetic simulations (μM) for the scenario 3, when a left-handed Neel domain wall is stabilized by the DMI and driven by the SHE in the absence of the Rashba and spin transfer torques.